Molecular Therapy
Methods & Clinical Development
Original Article

Comparison of analytical techniques to quantitate the capsid content of adeno-associated viral vectors

Amanda K. Werle,[1] Thomas W. Powers,[1] James F. Zobel,[1] Caitlin N. Wappelhorst,[1] Martin F. Jarrold,[2] Nicholas A. Lyktey,[2,3] Courtney D.K. Sloan,[1] Andrew J. Wolf,[1] Sharee Adams-Hall,[1] Phoebe Baldus,[1] and Herbert A. Runnels[1]

[1]Pfizer Inc., Analytical Research and Development, 875 Chesterfield Pkwy. West, Chesterfield, MO 63017, USA; [2]Indiana University, Chemistry Department, Bloomington, IN 47405, USA; [3]Gravity Diagnostics, Covington, KY 41011, USA

Adeno-associated virus (AAV) vectors, which contain a DNA transgene packaged into a protein capsid, have shown tremendous therapeutic potential in recent years. An inherent characteristic of the manufacturing process is production of empty capsids that lack the transgene and are therefore unable to provide the intended therapeutic benefit. The effect of empty capsids on clinical outcomes is not well understood, but there are immunogenicity and efficacy concerns, and these empty capsids are considered a product-related impurity. Therefore, empty capsids should be controlled during the manufacturing process and monitored through analytical testing, but there are limited techniques available that are capable of quantifying capsid content and even fewer that are amenable to validation and implementation as registered release tests in a regulated environment. In addition, there is currently not a widely accepted gold standard technique for quantifying capsid content, and the understanding of how the results compare between different orthogonal technologies is limited. The current study utilizes a comprehensive assessment to evaluate diverse analytical techniques for their ability to quantitate capsid content.

INTRODUCTION

Adeno-associated viruses (AAVs) have emerged as vectors of choice for gene therapy clinical trials because of their long-term expression and lack of pathogenicity in humans.[1] As a testament to the increased interest in and promise of AAV-based gene therapy products, the US Food and Drug Administration (FDA) has received a surge in the number of investigational new drug (IND) applications in recent years. In December 2017, they approved the first gene therapy product, Luxturna, for *RPE-65*-related inherited retinal diseases.[2] Although there are different processes for manufacturing AAV vectors, a common method is through plasmid DNA transfection of human embryonic kidney 293 (HEK293) cells using a vector construct plasmid containing the gene of interest and helper plasmid(s) containing the Ad5 genes and the AAV *Rep* and *Cap* genes.[3] The expressed forms of the *Rep* gene are necessary for genome replication and packaging, and the *Cap* gene is required for expression of three viral capsid proteins (VP1, VP2, and VP3) that form the AAV protein capsid. The AAV wild-type virus consists of a single-stranded DNA genome up to 4.8 kb in size that is flanked by inverted terminal repeats (ITRs), and this genome is encapsidated within a protein shell that is assembled from 60 proteins at a molar VP1:VP2:VP3 ratio of approximately 1:1:10.[4]

An inherent characteristic of the AAV manufacturing process is production of capsids that are not packaged with the therapeutic transgene and are therefore referred to as empty capsids. In general, up to 95% of the capsids produced upstream in the cell culture may be empty capsids, and this percentage has been shown to vary significantly between independent vector preparations.[5] In its natural life cycle, wild-type AAVs have also been shown to produce a large proportion of empty capsids.[6] The clinical effect of these empty capsids is not well understood, but it has been suggested that there could be elevated immune responses to high concentrations of viral particles and potential impairment of potency through receptor competition. Empty capsids are unable to provide the intended therapeutic benefit and are therefore considered to be a product-related impurity.[7,8] In addition to empty capsids, a heterogeneous population of partially-filled (or intermediate) capsids may also be produced during the manufacturing process, containing packaged process-related impurities or truncated genomes.[7,9] Therefore, it is essential to have analytical techniques that are capable of providing information regarding the content distribution of AAV capsids, referred to here simply as capsid content.

Several studies have evaluated analytical methods, individually or in tandem, for their ability to assess capsid content. Sommer et al.[10] demonstrated the ability to use ultraviolet (UV) absorbance, specifically the A_{260}/A_{280} ratio, which performs comparably to the ratio

Received 29 April 2021; accepted 25 August 2021;
https://doi.org/10.1016/j.omtm.2021.08.009.

Correspondence: Herbert A. Runnels, Pfizer Inc., Analytical Research and Development, 875 Chesterfield Pkwy. West, Chesterfield, MO 63017, USA.
E-mail: herbert.a.runnels@pfizer.com

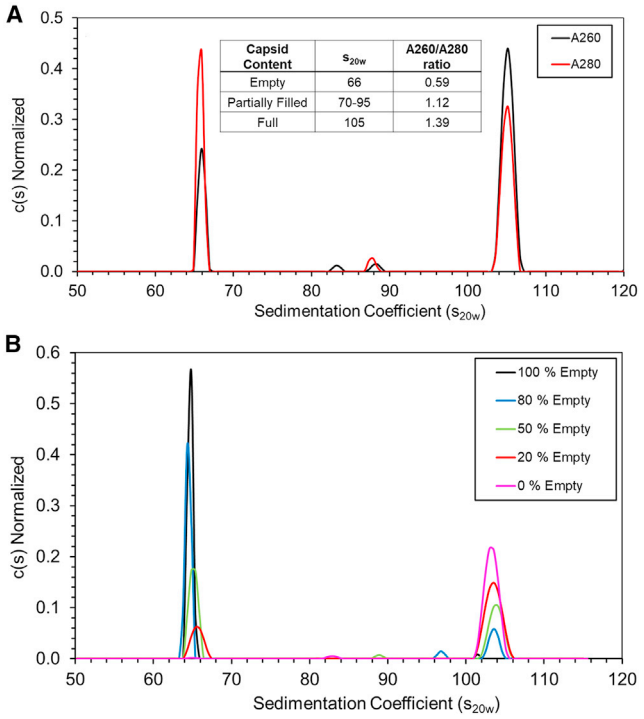

Figure 1. AUC Distribution plots for selected prepared spike ratio samples
(A) An overlay of AAV c(s) distribution plots from A_{260} and A_{280} Abs for empty, intermediate, and full capsids. (B) An overlay of AAV c(s) distribution plots from interference data for selected spike ratios ranging from 0% empty to 100% empty capsids. The profiles are color coded according to the key on the plot.

obtained from the independent capsid titer and genome titer assays. McIntosh et al.[11] detailed the use of size exclusion chromatography coupled to multiangle light scattering (SEC-MALS) to characterize capsid content in addition to other quality attributes. Density-based separation by analytical ultracentrifugation (AUC) has also been employed successfully to resolve empty, intermediate, and full capsids and to quantitate the approximate levels of each population.[12] Subramanian et al.[13] utilized a 2D and 3D classification process to visually identify and quantify empty, intermediate, and full capsids by cryoelectron microscopy (cryo-EM) and correlated the results to AUC. Using a mass-based separation of single intact capsids, Pierson et al.[14] successfully performed charge detection mass spectrometry (CDMS) to discriminate between empty, intermediate, and full capsids and generated data consistent with transmission electron microscopy (TEM).[14] Other laboratories have demonstrated the ability to use charge-based chromatographic separation based on differences in empty and full capsids to quantitate the empty-to-full capsid ratio.[15,16] In one instance, Fu et al.[17] developed a charge-based chromatography assay to quantify the empty-to-full capsid ratio and showed good comparability with AUC and TEM. The current study provides a controlled, comprehensive assessment of these orthogonal techniques with the goals of establishing a gold standard technique for capsid content quantification and developing a robust analytical control strategy for product release and characterization.

RESULTS

AUC-SV

AUC sedimentation velocity (AUC-SV) can be used to analyze capsid content through the difference in buoyant density between empty and full capsids. Figure 1A shows a representative overlay of the c(s) distribution plots derived from A_{260} and A_{280} absorbance scans as well as the average sedimentation coefficients and A_{260}/A_{280} ratios. Full capsids have a greater buoyant density than empty capsids and, therefore, sediment more quickly through solution. Full capsids have a sedimentation coefficient c(s) of approximately 105 s, whereas empty capsids have s values of approximately 66 s. Because the nucleic acid content of the capsid has a profound influence on the A_{260} and A_{280} absorbance data, the resulting A_{260}/A_{280} ratio for each species in the c(s) plot of the absorbance data can be used to support the identification of peaks in the c(s) plot. The A_{260}/A_{280} ratio is obtained by integrating the peak area of individual species in the c(s) plot at both wavelengths and dividing the A_{260} measurement by the A_{280} measurement. As shown in Figure 1A, full and empty capsids have ratios of 1.39 and 0.59, respectively. These data are consistent with the A_{260}/A_{280} ratio of the CsCl-enriched full and empty capsids determined spectrophotometrically and chromatographically, as illustrated in Table 1. An additional population of partially full capsids appears as multiple species with intermediate s values that range between 70–95 s and an average intermediate A_{260}/A_{280} ratio of 1.12 (Figure 1A).

Figure 1B shows select representative c(s) profiles from interference data for several prepared spike samples with variable capsid content. The interference data are used for quantitative analysis of the empty, intermediate, and full capsid distribution because the refractive index (RI) increment (dn/dc) is not significantly different between the different capsid species. Empty capsids have a dn/dc value of about 0.185, and full capsids have a predicted dn/dc value of about 0.181. The 2% difference in dn/dc value is within the typical variability of the method. Results for the prepared spike ratio samples are provided in Table 1. There is excellent agreement between the expected and the measured percentages of empty capsids determined by AUC. These results demonstrate that AUC is a powerful tool for direct quantitation of capsid content with an additional advantage of resolving intermediate capsids.

CDMS

CDMS can be used to analyze capsid content through the differences in charge and mass between empty and full capsids. CDMS is a single-capsid technique where the mass-to-charge ratio (m/z) and charge (z) are measured simultaneously and then multiplied to yield the mass of each ion.[14,18–24] Measurements are performed for thousands of ions, and the results are then binned to yield a mass spectrum. The detection efficiency is proportional to $(m/z)^{1/2}$ and so each ion is weighted by $(m/z)^{-1/2}$ to compensate when using CDMS for relative quantitation.

Figure 2 shows CDMS spectra measured for selected spike ratio samples ranging from 0%–100% empty capsids. There are two

Table 1. Data summary of capsid content determined by all orthogonal techniques assessed in comparison with the theoretical percentage of empty capsids in 11 prepared spike ratio samples across the empty-to-full capsid ratio range

Theoretical % empty	% empty by AUC	% empty by CDMS	% empty by cryo-EM	% empty by titer ratio	% empty by SEC-MALS	SEC A_{260}/A_{280}	UV A_{260}/A_{280}
100%	100%	100%	99%	100%	100%	0.58	0.58
91%	92%	91%	98%	93%	96%	0.76	0.75
83%	85%	84%	95%	87%	90%	0.87	0.86
80%	82%	79%	93%	88%	87%	0.91	0.90
75%	76%	78%	92%	85%	81%	0.97	0.95
67%	69%	68%	85%	76%	75%	1.06	1.03
50%	55%	49%	74%	64%	58%	1.17	1.16
33%	41%	38%	67%	47%	40%	1.27	1.26
20%	23%	18%	51%	36%	24%	1.32	1.32
9%	10%	8%	34%	25%	9%	1.36	1.36
0%	3%	0%	14%	15%	0%	1.39	1.39

prominent peaks at around 3.8 MDa and 5.3 MDa that are attributed to empty and full capsids, respectively. Figure 2B shows CDMS spectra for the 100% empty and 0% empty samples with an expanded vertical scale. These data also confirm efficient enrichment of capsids in the starting material, showing almost entirely empty capsids in the 100% empty sample (black spectrum) and undetectable levels of empty capsids in the 0% empty sample (pink spectrum). For the 0% empty sample, there is significant intensity at around 4.9 MDa, which is smaller than the expected mass of the full capsid. This species is likely due to the presence of intermediate capsids. There is virtually no intensity at intermediate masses for the 100% empty sample (black spectrum), suggesting that the intermediate capsids are primarily co-purified with the full capsids.

The peaks for the 0% empty and 100% empty samples in Figure 2A have different amplitudes. This is partly due to the intermediate intensity (which amounts to around 6% for the 0% empty sample) and partly due to the inherent heterogeneity of the 0% empty peak being slightly broader than the 100% empty peak. Additional spike ratios are plotted in Figure 2A to demonstrate the feasibility of using CDMS to quantify the fraction of empty capsids. To process the data for relative quantitation, empty capsids were defined by the mass range between 3.5 and 4.0 MDa, and full capsids were defined by the mass range between 4.0 and 5.5 MDa (intermediate capsids are included with full capsids, as indicated in Figure 2B). Relative quantitation was performed by dividing the integrated intensity of the empty capsids by the sum of the integrated intensities of the full and empty capsids. Results for the 11 prepared spike ratio samples are shown in Table 1. There is excellent agreement between the theoretical spike sample percentages and the percentages of empty capsids detected by CDMS. These results indicate that CDMS is a valuable tool for quantitation of capsid content, and it can also be used to gain information about the mass population of intermediate capsids.

Cryo-EM

Cryo-EM can be used to determine capsid content by distinguishing empty and full capsids through image density analysis. Cryo-EM, as opposed to negative-stain TEM, was included in this study because it removes the variability introduced by inconsistent staining of capsids across the grid as well as potential artifacts associated with the precipitation of the stain. As shown in Figure 3A, full capsids display an inner density with no distinct boundary between the shell and core of the capsid, whereas empty capsids display a distinct outer shell and minute internal density. Principal-component analysis of each AAV capsid's radial density profile reveals a separable clusters plot corresponding to the level of packaging, with packaging statistics (Figure 3B) showing the relative abundance of each distinct population from multiple images of more than 1,000 total capsids. Results for the 11 prepared spike ratio samples are shown in Table 1. There is an overestimation of empty capsids in comparison with the expected percentage of empty capsids across the empty-to-full capsid ratio range.

A_{260}/A_{280} ratio

UV absorbance can distinguish between capsids containing packaged DNA and empty capsids based on the intrinsic chromophore absorption characteristics of DNA and proteins. DNA has a maximum absorbance at 260 nm because of the aromatic nitrogen rings in its structure, and proteins have a maximum absorbance at 280 nm because of the aromatic residues in the peptide sequence. Utilizing these absorbance characteristics, a capsid content ratio can be calculated from the primary absorbance of the vector genome at 260 nm and the capsid proteins at 280 nm. Because of the significant interference absorbance of DNA at 280 nm, data acquired from direct measurement techniques (i.e., AUC, CDMS) are required to appropriately interpret the A_{260}/A_{280} ratio.

The A_{260}/A_{280} method can be performed spectrophotometrically (UV A_{260}/A_{280}) and chromatographically (SEC A_{260}/A_{280}). Using a

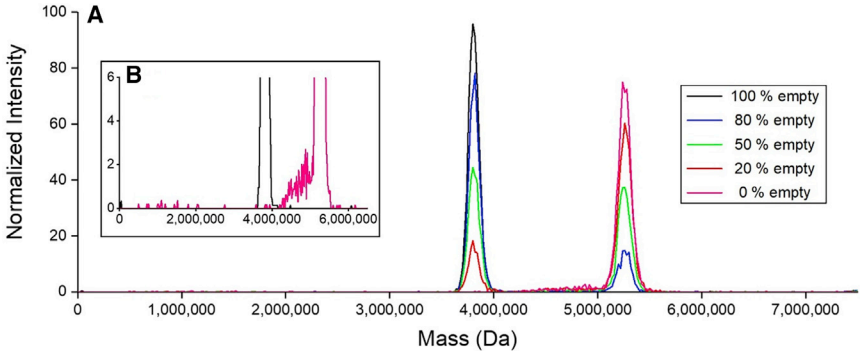

Figure 2. Normalized CDMS spectra for selected spike ratios

The spectra are plotted using 20-kDa bins. (A) CDMS spectra measured for selected spike ratios ranging from 0% empty to 100% empty. The spectra are color coded according to the key given on the right of the plot. (B) CDMS spectra for the 100% empty capsid (black) and 0% empty capsid (pink) with an expanded vertical scale. There are capsids associated with the 0% empty capsid sample that have masses between the peaks attributed to the empty and full capsids.

spectrophotometer, the UV A_{260}/A_{280} ratio is calculated by subtracting A_{320} from A_{260} and A_{280} as a scatter correction and then dividing A_{260} by A_{280}. Using SEC, AAV capsids elute as a single peak under isocratic conditions regardless of capsid content. Chromatograms of AAV capsids are collected at multiple wavelengths, and the peak area ratio is determined by dividing the capsid peak area at 260 nm by the capsid peak area at 280 nm. Both A_{260}/A_{280} ratio methods exhibit excellent agreement between each other across the empty-to-full capsid ratio range (Table 1). The enriched empty sample has a ratio of approximately 0.58, whereas the enriched full sample has a ratio of approximately 1.39. These A_{260}/A_{280} ratios demonstrate excellent agreement with the A_{260}/A_{280} ratios for empty and full capsids determined by AUC, which are 0.59 and 1.39, respectively, in Figure 1A. UV A_{260}/A_{280} ratio and SEC A_{260}/A_{280} ratio measurements for the 11 prepared spike ratio samples are shown in Table 1. Both A_{260}/A_{280} ratio curves are nonlinear, but a correlation plot between the A_{260}/A_{280} ratio and the percentage of empty capsids calculated by a suitable direct measurement technique can be used to interpolate a percent empty capsid result from the A_{260}/A_{280} ratio value (Figure 4).

SEC with UV, MALS and RI

SEC-MALS can be used to determine capsid content by distinguishing the protein and nucleic acid contribution of the AAV capsid for molar mass and eluted mass. The dn/dc values are well known for the respective class of molecules, and the extinction coefficients used for the AAV capsid and DNA at UV_{260} were provided by Wyatt Technology based upon empirical determination for AAV samples. These values are used in the ASTRA Protein Conjugate Analysis module to calculate the contribution of each component with respect to molar mass (MDa) and eluted mass (μg). Molar masses measured from the 0% empty sample include total mass, protein capsid mass, and DNA mass, calculated as 5.0 MDa, 3.7 MDa, and 1.3 MDa, respectively. Molar masses measured from the 100% empty sample include total mass (i.e., protein capsid mass), calculated as 3.8 MDa (Figure 5). These calculated mass values agree with the theoretical values based on the protein and DNA sequences and the structure of the AAV capsid; the results also align with the mass values obtained by CDMS. The Protein Conjugate Analysis module can also combine the eluted mass with molar mass to calculate quality attributes such as capsid titer and capsid content.

Total capsid concentration is determined using Equation 1:

$$C_{AAV} = m_P \times N_A / \left(M_{Capsid} \times \upsilon\right), \quad \text{(Equation 1)}$$

where C_{AAV} is the total capsid concentration, m_P is the total eluted protein mass, N_A is Avogadro's number, M_{Capsid} is the capsid's molar mass, and υ is the injected volume of the test sample. For the enriched empty and full samples used in this study, the total capsid concentration values, as determined by SEC-MALS, are 4.89E13 capsids/mL and 3.61E13 capsids/mL, respectively. The concentration of full capsids is determined using Equation 2:

$$C_{full} = m_{DNA} \times N_A / \left(M_{Full} \times \upsilon\right), \quad \text{(Equation 2)}$$

where C_{full} is the full capsid concentration, m_{DNA} is the total eluted DNA mass, N_A is Avogadro's number, M_{Full} is the encapsidated DNA's molar mass, and υ is the injected volume of the test sample. After determining the total and full capsid concentrations, the concentration of empty capsids is determined using Equation 3,

$$C_{empty} = C_{AAV} - C_{full}. \quad \text{(Equation 3)}$$

Capsid content is calculated using the C_{AAV} and C_{empty} values, where the percentage of empty capsids is determined using Equation 4:

$$\%\ \text{Empty} = C_{empty} / C_{AAV} \times 100\%. \quad \text{(Equation 4)}$$

Results for the 11 prepared spike ratio samples are shown in Table 1. There is good agreement between the theoretical spike sample percentages and the percentages of empty capsids quantified by SEC-MALS. These results demonstrate that SEC-MALS is a promising technique for determination of capsid content.

Capsid titer-to-genome titer ratio

The capsid titer-to-genome titer ratio method can be used to determine capsid content by distinguishing empty and full capsids through independent capsid and genome titer measurements. Capsid titer is quantified by SEC, and genome titer is determined by qPCR; the percentage of empty capsids for each test sample was calculated using the equation $100 \div \frac{\text{Capsid titer}}{\text{Genome titer}}$. Results for the 11 prepared spike ratio samples are shown in Table 1. There is an overestimation of empty

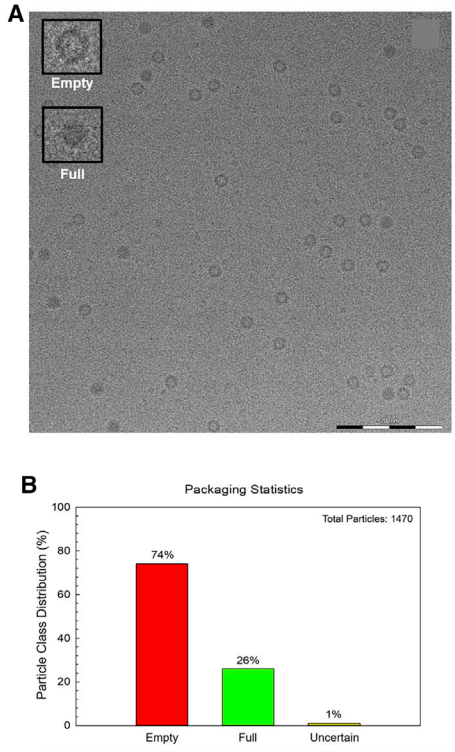

Figure 3. Cryo-EM analysis of 50% empty spike sample

(A) Cryo-EM for the 50% empty AAV capsid sample shown at 38,000× magnification, where the approximate capsid diameter is measured to be 22 nm. Representative images are shown for "empty" and "full" capsids in the top left panel. "Empty" capsids display a distinct outer shell and minute internal density, whereas "full" capsids have an inner density with no distinct boundary between the shell and core. (B) Packaging statistics for the sample imaged in Figure 3A, after images undergo capsid detection and classification by internal density analysis. Radial density profiles of sample capsids showed two major classes of capsid packaging.

capsids in comparison with the expected percentage of empty capsids across most of the empty-to-full capsid ratio range.

DISCUSSION

In the current study, several analytical techniques were assessed for their ability to quantitate capsid content using a well-controlled preparation of spike ratio samples. Other analytical techniques have also demonstrated this capability but were not included in this study. For example, several publications have demonstrated the ability to use charge-based chromatographic separation for determining capsid content,[15,16] but this approach appears to be serotype specific and could not be applied in this study for the proprietary serotype (data not shown). All of the techniques evaluated in the current study were tested successfully across at least three unique AAV serotypes (data not shown). It is important to note that the conclusions drawn from the assessment of these techniques remain robust and consistent across multiple materials tested to date, including variations in AAV serotypes, genome lengths, and differential placement of the amplicon used for viral genome titration. With this knowledge, we find

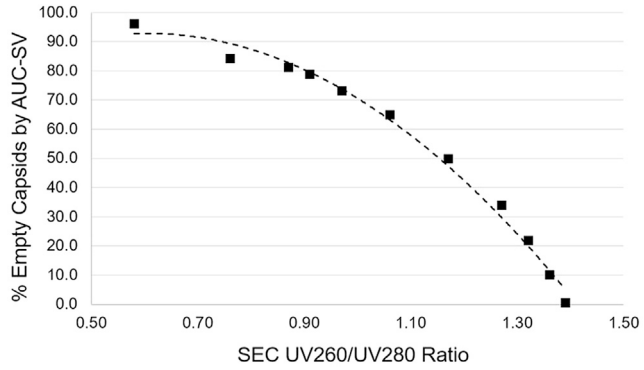

Figure 4. Correlation plot between AUC-SV and SEC A_{260}/A_{280} ratio for spike ratios ranging from 0% empty to 100% empty capsids, which can be used to interpolate a percent empty capsid result from the A_{260}/A_{280} ratio value

these conclusions to be a reproducible assessment and not necessarily affected by typical analytical variations, but careful consideration should be given to each particular program when implementing a particle content testing strategy. Although some methods performed better than others, the experimental results from each analytical technique overall trended relatively well with the theoretical percentages of empty capsids, as illustrated in Figure 6. The experimental results for AUC, CDMS, SEC-MALS, and titer ratio were analyzed using a linear best fit line; however, the SEC A_{260}/A_{280} ratio, UV A_{260}/A_{280} ratio, and cryo-EM results were best fit using a polynomial curve.

AUC and CDMS quantify the expected capsid content with high accuracy relative to the theoretical spiked levels (Table 1; Figure 6) and therefore are considered to be gold standard methods from a characterization perspective. In addition to quantification of capsid content, both techniques have additional utilities. For example, AUC is able to report the A_{260}/A_{280} ratios for individual species across the sedimentation profile, which can provide orthogonal supportive data to the spectrophotometric and chromatographic ratio measurements as well as potentially provide insight regarding the capsid content of the intermediate species. In our experience, the A_{260}/A_{280} ratios for enriched empty and full capsid samples obtained by AUC match the expected A_{260}/A_{280} ratios from the SEC and UV A_{260}/A_{280} methods for enriched empty and full capsids (Table 1). CDMS, on the other hand, enables an analyst to obtain the mass information for empty and full capsids, which can then be used to identify the mass of the packaged DNA. Furthermore, AUC (Figure 1) and CDMS (Figure 2) are able to resolve intermediate density and mass species, respectively. Although these techniques are considered by us to be analytical gold standards for capsid content characterization, they have several limitations that prevent broader use, particularly in quality control (QC) laboratories that perform current good manufacturing practices (cGMP) testing for product release (Table 2). These limitations include relatively low throughput data acquisitions, non-cGMP compliance concerns related to instrument-specific acquisition software, and

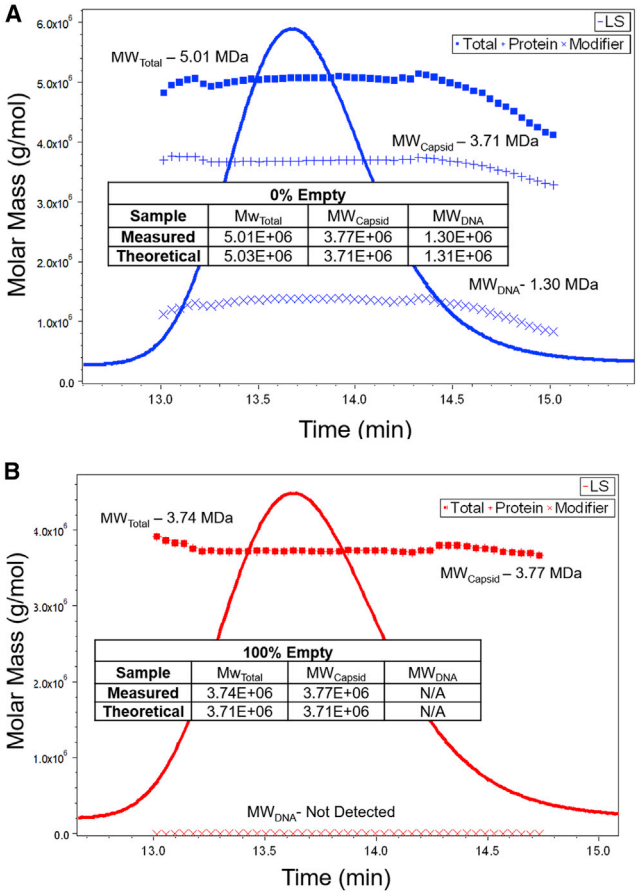

Figure 5. SEC-MALS analysis of 0% and 100% empty spike samples

(A) Molar masses measured from the 0% empty sample, showing total mass (squares) of 5.0 MDa, protein capsid mass (+ symbols) of 3.8 MDa, and DNA mass (x symbols) of 1.3 MDa overlaid with the light scattering chromatogram. (B) In the 100% empty sample, the molar mass of an "empty" capsid is calculated to be 3.8 MDa.

use of specialized equipment, particularly for CDMS, which is in nascent stages of instrument commercialization.

Although use of cryo-EM for quantitation of capsid content was not highly accurate across the spike range in our study, cryo-EM continues to be a very useful technique for characterization of AAV. For example, Subramanian et al.[13] found very good cross-correlation of AUC and cryo-EM on sample sets that have a majority of capsids classified as empty. Our study extends their work by examining the correlation across a wider range of empty capsids and finds that the correlation between AUC and cryo-EM is less optimal, with a greater overestimation of percent empty in capsids when the overall capsid population has a lower percentage of empty capsids (i.e., a higher percentage of full capsids). Furthermore, among the various techniques that were assessed, cryo-EM is unique in that enables direct visualization of the AAV capsid, which is useful in demonstrating the size and shape of the assembled capsid. Overall, the results did trend as expected with increasing levels of empty capsids, but it appeared to overestimate the percentage of empty capsids across most of the spike range. It is possible that adjustments could be made to the software to improve the capsid detection and classification algorithms and thereby enhance the accuracy of the technique for quantifying capsid content. As the technique stands currently, its ability to distinguish intermediate capsids from empty and full capsids has not been established.

AUC, CDMS, and cryo-EM are excellent characterization tools but are less suitable for implementation in a cGMP laboratory environment in comparison with other test options. As part of our orthogonal assessment, other techniques were evaluated that utilize data acquisition programs and instrumentation that are more appropriate for routine testing as part of product release. These techniques include genome titer-to-capsid titer ratio, UV A_{260}/A_{280}, SEC A_{260}/A_{280}, and SEC-MALS. The titer ratio is determined by a simple calculation and can be obtained without running any additional experiments because the genome titer and capsid titer methods are generally deployed as part of product release testing. In our study, the titer ratio results demonstrate a linear correlation with the percentage of empty capsids, but this approach appears to overestimate the percentage of empty capsids across much of the spike range. In addition, a primary limitation with this technique stems from compounding variability resulting from the reliance on two independent methods. The A_{260}/A_{280} ratio methods provide an indirect but high-throughput option for assessing capsid content. As indicated earlier, the primary limitation with this approach is that it requires correlative data from a direct measurement technique to interpret the A_{260}/A_{280} ratio. Although both A_{260}/A_{280} assays can be used to monitor the overall consistency of the percentage of empty capsids produced by the manufacturing process, they cannot resolve intermediate capsids. SEC A_{260}/A_{280} offers an advantage over UV A_{260}/A_{280} because of its ability to chromatographically resolve intact AAV capsids from sample-related impurities. In addition, SEC can be coupled to other detectors to assess multiple quality attributes. For example, SEC-MALS can be used to determine capsid and genome concentration, size distribution, capsid content, and capsid molar mass.[11] In our study, the percentage of empty capsids quantified by SEC-MALS demonstrated great correlation to the theoretical spiked levels across the empty-to-full ratio range; however, SEC-MALS is not able resolve intermediate capsids. In conclusion, various analytical techniques have been assessed for their ability to accurately distinguish and quantitate full, intermediate, and empty capsids, but the advantages and disadvantages, as described in Table 2, of each method should be considered when choosing the most technique most suitable for the objective. Appropriate utilization of these diverse tools enables analysis of the capsid content across the manufacturing process to improve process understanding and to monitor batch consistency and quality between manufactures.

MATERIALS AND METHODS

Vector production, purification, and preparation for analysis

AAV vectors were produced through triple transfection of adherent HEK293 cells. The intended product is a therapeutic transgene

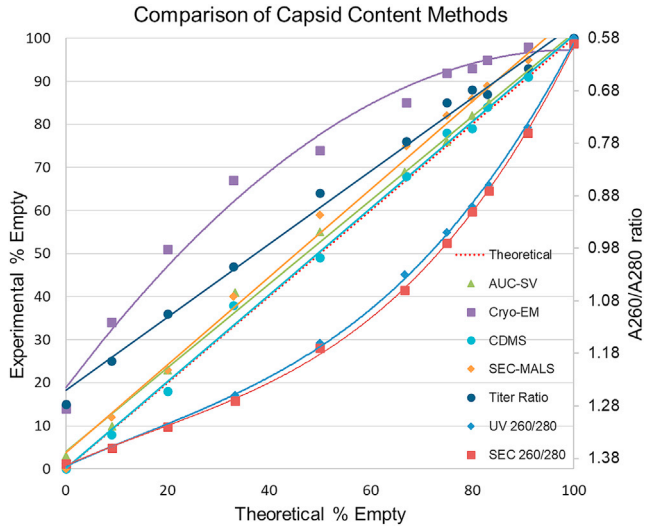

Figure 6. Data comparison of capsid content determined by orthogonal techniques in comparison with the theoretical percentage of empty capsids in 11 prepared spike ratio samples across the empty-to-full capsid ratio range.

sequence flanked by AAV2 ITRs encapsidated by an engineered viral capsid with a proprietary protein sequence. The crude harvest material was clarified by filtration and purified by ion exchange (IEX) chromatography. Enriched empty and full samples were generated via cesium chloride ultracentrifugation using a Beckman Coulter Optima XPN-80 ultracentrifuge with a SW 40Ti swinging bucket rotor run at 40,000 rpm for 44 h at 15°C. The IEX eluate was concentrated approximately 2-fold and mixed directly with CsCl powder to generate an AAV-containing 3M CsCl solution. Following centrifugation, two distinct viral bands were visible: a low-density and high-density band corresponding to empty and full capsids, respectively. Each purified band was collected via side puncture and dialyzed into a Tris/NaCl buffer. The capsid concentration of each bulk enriched fraction was determined by SEC, followed by subsequent dilution in a proprietary formulation buffer to a final capsid concentration of 3.0E13 capsids/mL. The diluted enriched samples were then mixed at various ratios to prepare test samples across the empty-to-full range. The expected percentage of empty capsids for the prepared spike ratio samples are as follows: 0% empty, 9% empty, 20% empty, 33% empty, 50% empty, 67% empty, 75% empty, 80% empty, 83% empty, 91% empty, and 100% empty. All prepared spike ratio samples were tested using each analytical technique described below.

AUC-SV

The test samples were diluted 1:3 into proprietary formulation buffer and analyzed using a Beckman Coulter Optima analytical ultracentrifuge run at 15,000 rpm at 20°C. Absorbance data were collected at wavelengths of 260 and 280 nm every minute for a total of 100 scans for each wavelength. Interference data were collected every minute for a total of 200 interference scans. The resulting data were analyzed using Sedfit (v.15.01b) to generate c(s) size distribution plots for each of the three data collection methods. Sednterp (v.1.09) was used to determine the solvent viscosity (0.01023 Poise) and density (1.00709 g/mL). An average partial specific volume of 0.7093 mL/g for the AAV capsid was used for the analysis.

CDMS

The prototype CDMS instrument, methods,[18–20] and data analysis[21,22] have been described in detail elsewhere. Briefly, test samples were buffer exchanged into a 100-mM ammonium acetate buffer (pH 7.5) using Micro Bio-Spin columns (Bio-Rad). Ions were produced by a nano-electrospray source (Advion Biosciences), introduced into the instrument through a heated metal capillary, and passed through an ion funnel, a hexapole ion guide, and a quadrupole ion guide. They were then focused into a dual hemispherical deflection energy analyzer (HDA), which transmits ions within a narrow band of kinetic energies centered on 100 electronvolt (eV)/z. The transmitted ions were focused into an electrostatic linear ion trap with a cylindrical charge detector tube at its center. Individual ions are trapped for 100 ms, during which the ion oscillates back and forth through the detector tube, inducing a periodic signal that is amplified, digitized, and transferred to a computer for analysis. The digitized signals were analyzed by a Fortran program using fast Fourier transforms. Results were only retained from trapping events where a single ion was trapped for the full trapping period; other trapping events were discarded.

Cryo-EM

The test samples were added neat to a continuous carbon grid that had been glow discharged using a Pelco easiGlow. The coated grid was frozen in liquid ethane and imaged using a Talos L120C microscope (at 120 kV) and a Thermo Fisher Scientific Ceta 16M detector. Images were collected at 38,000× and 57,000× times magnification. Data analysis was performed using VAS analytical software (Vironova, Stockholm, Sweden), which performed an internal density analysis to classify capsids as "empty," "full," and "uncertain" based on capsid radial density profiles, followed by a principal-component analysis to determine the relative abundance of each capsid population.

qPCR

Test samples were analyzed for genome titer using qPCR technology. AAV samples were treated with DNase I (Invitrogen) at 37°C for 1 h to digest non-packaged DNA followed by treatment with SDS/EDTA/NaCl solution, heated to inactivate the DNase I enzyme, and denature the viral capsid. Test samples were then diluted into the assay range for analysis. A standard curve was prepared by serial dilution of linearized plasmid containing the transgene with a known copy number. After addition to the reaction plate, qPCR Master Mix (Applied Biosystems) containing target-specific primers and a TaqMan probe were added to each well. Samples were analyzed on an Applied Biosystems 7500 real-time PCR system, and the concentration of the target sequence was interpolated from the standard curve and subsequently converted to vector genomes (vgs) per milliliter.

Table 2. Summary of advantages and disadvantages associated with each technique assessed in the current study

AUC-SV	CDMS	Cryo-EM	UV A_{260}/A_{280}	SEC A_{260}/A_{280}	SEC-MALS	Titer ratio
Advantages						
• relative quantitation of capsid content • resolves intermediate mass species • provides A_{260}/A_{280} ratios for individual species	• relative quantitation of capsid content • resolves intermediate mass species • provides mass and charge of capsid populations • low material requirements	• relative quantitation of capsid content • low material requirements • provides capsid size and shape through direct visualization	• high throughput • easily implemented technology • low material requirements • implementable in a cGMP environment	• high throughput • easily implemented technology • resolves capsid from impurities • low material requirements • implementable in a cGMP environment	• high throughput • easily implemented technology • low material requirements • provides capsid aggregate, concentration, molar mass, and size • implementable in a cGMP environment	• easily implemented technology • utilizes existing data from routinely performed assays • implementable in a cGMP environment
Disadvantages						
• relatively large material requirement • low throughput • requires specialized equipment • challenging to implement in cGMP environment	• low throughput • requires specialized equipment • challenging to implement in cGMP environment	• low throughput • intermediate species not quantified • requires specialized equipment • challenging to implement in cGMP environment	• indirect measurement of capsid content • potential interference from impurities • cannot resolve intermediate species	• indirect measurement of capsid content • cannot resolve intermediate species	• cannot resolve intermediate species • assumes 100% mass recovery from SEC column • assumes use of appropriate extinction coefficient	• indirect measurement of capsid content • compounding variability due to a ratio of two independent methods • cannot measure intermediate species

SEC

The test samples were injected neat onto a TOSOH TSKgel column and separated by isocratic elution using a phosphate-buffered mobile phase. The detection system was comprised of an Agilent 1200 series high performance liquid chromatography (HPLC) system with a UV-visible (UV-vis) diode array detector collecting at UV wavelengths of 214, 260, and 280 nm. The capsid titer (capsids per milliliter) values of the enriched empty and full fractions and prepared spike ratio samples were determined using relative peak area quantitation at 214 nm against a calibration curve prepared with an AAV standard of a predetermined concentration. SEC separates components by hydrodynamic volume, resulting in elution of AAV capsids at a consistent retention time regardless of the packaged content. This technique was also utilized to assess the capsid content through a 260/280 peak area ratio calculation. The chromatographic peak corresponding to the AAV monomer was integrated at 260 nm and 280 nm, and the peak area ratio (SEC A_{260}/A_{280} ratio) was calculated for each sample.

UV spectroscopy

Test samples were measured neat in a quartz cuvette (Starna Cells) at UV wavelengths of 260 nm, 280 nm, and 320 nm. A matching formulation buffer blank was used to zero the instrument before each sample measurement, and each wavelength was read for 0.5 s. A Cary 60 UV-vis spectrophotometer employs a light source shining through a monochromator and a detector to determine the absorbance (Abs) of a sample as a function of percent transmittance (%T) at a specific wavelength. As the spectrophotometer emits UV light, the monochromator selects the chosen wavelength to allow it to pass through the sample. The detector quantifies the photons passing through the sample as percent transmittance, which is calculated to Abs by the function $Abs = 2 - \log_{10}(\%T)$. A_{320} was subtracted from A_{260} and A_{280} as a scatter correction, and then the corrected A_{260} was divided by the corrected A_{280} to calculate the UV A_{260}/A_{280} ratio.

SEC with UV, MALS and RI

The test samples were injected neat onto a Wyatt WTC-050S5 column at a load of 5 μg and separated by isocratic elution using a phosphate-buffered mobile phase. The detection system was comprised of an Agilent 1200 series HPLC system with a UV-vis diode array detector collecting at UV wavelengths of 260 and 280 nm, a Wyatt Dawn Heleos II MALS detector, and an Optilab T-rEX dRI detector. The total and full capsid titers of the test samples were determined using the Protein Conjugate Analysis feature of Wyatt's ASTRA software. The calculated values of these attributes were used to calculate capsid content. These calculations were performed using distinct dn/dc values for protein and DNA of 0.185 and 0.170 mL/g, respectively, and distinct UV extinction coefficients for protein capsid and DNA of 1.3 and 24 mL/mg·cm, respectively.

Capsid titer-to-genome titer ratio

Test samples were analyzed by qPCR to determine the genome titer and SEC to determine the capsid titer. The percentage of

empty capsids for each test sample was calculated using the following equation:

$$100 \div \frac{\text{Capsid titer}}{\text{Genome titer}}.$$

ACKNOWLEDGMENTS

Funding for this study was provided entirely by Pfizer Inc. We would like to acknowledge Tihami Qureshi, John Amery, Qin Zou, and Nathan Lacher from Pfizer Inc. for the technical review of the manuscript. We would like to acknowledge Stanley Dai and Joseph Binder from Pfizer Inc. for assistance with preparation of enriched fractions by cesium chloride ultracentrifugation. We would like to acknowledge Vironova for testing support by cryo-EM and Wyatt Technology for support with SEC-MALS.

AUTHOR CONTRIBUTIONS

A.K.W. conceived the idea for the study. A.K.W., T.W.P., P.B., and H.A.R. designed the study. T.W.P., J.F.Z., C.N.W., M.F.J., N.A.L., C.D.K.S., A.J.W., and S.A. generated materials, authored protocols, performed experiments, and analyzed data. A.K.W. and T.W.P. led authoring of the manuscript. J.F.Z., C.N.W., M.F.J., N.A.L., C.D.K.S., A.J.W., and S.A.-H. also contributed to the manuscript content and generated figures. All authors reviewed, edited, and approved the article.

DECLARATION OF INTERESTS

The authors declare no competing interests.

REFERENCES

1. Daya, S., and Berns, K.I. (2008). Gene therapy using adeno-associated virus vectors. Clin. Microbiol. Rev. *21*, 583–593.
2. Smalley, E. (2017). First AAV gene therapy poised for landmark approval. Nat. Biotechnol. *35*, 998–999.
3. Clément, N., and Grieger, J.C. (2016). Manufacturing of recombinant adeno-associated viral vectors for clinical trials. Mol. Ther. Methods Clin. Dev. *3*, 16002.
4. Samulski, R.J., and Muzyczka, N. (2014). AAV-Mediated gene therapy for research and therapeutic purposes. Annu. Rev. Virol. *1*, 427–451.
5. Wright, J.F. (2008). Manufacturing and characterizing AAV-based vectors for use in clinical studies. Gene Ther. *15*, 840–848.
6. Wright, J.F. (2009). Transient transfection methods for clinical adeno-associated viral vector production. Hum. Gene Ther. *20*, 698–706.
7. Wright, J.F. (2014). Product-related impurities in clinical-grade recombinant AAV vectors: Characterization and risk assessment. Biomedicines *2*, 80–97.
8. Wright, J.F. (2014). AAV empty capsids: for better or for worse? Mol. Ther. *22*, 1–2.
9. Wu, Z., Yang, H., and Colosi, P. (2010). Effect of genome size on AAV vector packaging. Mol. Ther. *18*, 80–86.
10. Sommer, J.M., Smith, P.H., Parthasarathy, S., Isaacs, J., Vijay, S., Kieran, J., Powell, S.K., McClelland, A., and Wright, J.F. (2003). Quantification of adeno-associated virus particles and empty capsids by optical density measurement. Mol. Ther. *7*, 122–128.
11. McIntosh, N.L., Berguig, G.Y., Karim, O.A., Cortesio, C.L., De Angelis, R., Khan, A.A., Gold, D., Maga, J.A., and Bhat, V.S. (2021). Comprehensive characterization and quantification of adeno associated vectors by size exclusion chromatography and multi angle light scattering. Sci. Rep. *11*, 3012.
12. Burnham, B., Nass, S., Kong, E., Mattingly, M., Woodcock, D., Song, A., Wadsworth, S., Cheng, S.H., Scaria, A., and O'Riordan, C.R. (2015). Analytical ultracentrifugation as an approach to characterize recombinant adeno-associated viral vectors. Hum. Gene Ther. Methods *26*, 228–242.
13. Subramanian, S., Maurer, A.C., Bator, C.M., Makhov, A.M., Conway, J.F., Turner, K.B., Marden, J.H., Vandenberghe, L.H., and Hafenstein, S.L. (2019). Filling adeno-associated virus capsids: Estimating success by cryo-electron microscopy. Hum. Gene Ther. *30*, 1449–1460.
14. Pierson, E.E., Keifer, D.Z., Asokan, A., and Jarrold, M.F. (2016). Resolving adeno-associated viral particle diversity with charge detection mass spectrometry. Anal. Chem. *88*, 6718–6725.
15. Lock, M., Alvira, M.R., and Wilson, J.M. (2012). Analysis of particle content of recombinant adeno-associated virus serotype 8 vectors by ion-exchange chromatography. Hum. Gene Ther. Methods *23*, 56–64.
16. Qu, G., Bahr-Davidson, J., Prado, J., Tai, A., Cataniag, F., McDonnell, J., Zhou, J., Hauck, B., Luna, J., Sommer, J.M., et al. (2007). Separation of adeno-associated virus type 2 empty particles from genome containing vectors by anion-exchange column chromatography. J. Virol. Methods *140*, 183–192.
17. Fu, X., Chen, W.C., Argento, C., Clarner, P., Bhatt, V., Dickerson, R., Bou-Assaf, G., Bakhshayeshi, M., Lu, X., Bergelson, S., and Pieracci, J. (2019). Analytical strategies for quantification of adeno-associated virus empty capsids to support process development. Hum. Gene Ther. Methods *30*, 144–152.
18. Fuerstenau, S.D., and Benner, W.H. (1995). Molecular weight determination of megadalton DNA electrospray ions using charge detection time-of-flight mass spectrometry. Rapid Commun. Mass Spectrom. *9*, 1528–1538.
19. Contino, N.C., and Jarrold, M.F. (2013). Charge detection mass spectrometry for single ions with a limit of detection of 30 charges. Int. J. Mass Spectrom. *345*, 153–159.
20. Contino, N.C., Pierson, E.E., Keifer, D.Z., and Jarrold, M.F. (2013). Charge detection mass spectrometry with resolved charge states. J. Am. Soc. Mass Spectrom. *24*, 101–108.
21. Pierson, E.E., Keifer, D.Z., Contino, N.C., and Jarrold, M.F. (2013). Probing higher order multimers of pyruvate kinase with charge detection mass spectrometry. Int. J. Mass Spectrom. *337*, 50–56.
22. Pierson, E.E., Contino, N.C., Keifer, D.Z., and Jarrold, M.F. (2015). Charge detection mass spectrometry for single ions with an uncertainty in the charge measurement of 0.65 e. J. Am. Soc. Mass Spectrom. *26*, 1213–1220.
23. Keifer, D.Z., Shinholt, D.L., and Jarrold, M.F. (2015). Charge detection mass spectrometry with almost perfect charge accuracy. Anal. Chem. *87*, 10330–10337.
24. Keifer, D.Z., Pierson, E.E., and Jarrold, M.F. (2017). Charge detection mass spectrometry: weighing heavier things. Analyst (Lond.) *142*, 1654–1671.